Analysis of Induction Skull Melting Furnace by Edge Finite Element Method Excited from Voltage Source

Vlatko Čingoski
Hideo Yamashita

Reprinted from
IEEE TRANSACTIONS ON MAGNETICS
Vol. 30, No. 5, September 1994

Analysis of Induction Skull Melting Furnace by Edge Finite Element Method Excited from Voltage Source

Vlatko Čingoski† Hideo Yamashita
Electric Machinery Laboratory, Faculty of Engineering
Hiroshima University, Kagamiyama 1-4
Higashi-hiroshima, 724 JAPAN

ABSTRACT – **To optimize the production of high-efficiency induction skull melting furnace, we analyzed magnetic flux density, eddy current and electromagnetic force distributions using the 3D edge-based finite element method excited from a voltage source. Changing the number of copper rods and, therefore, the distance between them, we analyzed both the intensity and direction of the electromagnetic forces and the amount of power consumed by the molten alloy and the rods. In this paper, we present our analysis method, the obtained results and conclusions.**

I. INTRODUCTION

To aid in the design and development of electromagnetic heat devices, a variety of numerical simulation methods have been researched [1]. To obtain precise output information in the design process, it is essential that designers employ precise numerical input information. Producing a high-efficiency induction skull melting furnace requires optimization of the furnace shape, and from an electromagnetic standpoint, other factors such as supplied voltage and frequency, number of turns in the coil and its current value, input power, and energy loss. Creating a physical model of the furnace requires 3D eddy current analysis, making optimization a complex process. Due to lengthy computation time, high memory requirements and an unknown preliminary source current value, the conventional nodal finite element method is obviously not the ideal solution. A new edge-based finite element method, however, has recently become an attractive solution for the wide-range of 3D electromagnetic field problems because of its short computation time and low memory requirements. Also, because the induction skull melting furnace is supplied with a constant and known voltage source determined by its electrical system, we adopted the supplied voltage as a source in the edge-based finite element method, creating a new and powerful tool for analyzing various 3D electromagnetic field problems.

In this paper, we apply the time-periodic edge-based finite element analysis excited from a voltage source using first-order tetrahedra to optimize a high-efficiency induction skull melting furnace.

Manuscript received November 1, 1993.

†The author is on leave from Electrotechical Faculty, University "Sv. Kiril i Metodij", Skopje, Macedonia

II. ANALYSIS APPROACH

3-D electromagnetic fields with eddy currents are governed by the following partial differential equations

$$rot\,(\nu\, rot\mathbf{A}) = \mathbf{J}_0 - \sigma\,(\frac{d\mathbf{A}}{dt} + grad\phi) \qquad (1)$$

$$div\,[-\sigma\,(\frac{d\mathbf{A}}{dt} + grad\phi)] = 0\,, \qquad (2)$$

where $\mathbf{A}$ and ϕ are the magnetic vector potential and electric scalar potential, respectively, $\mathbf{J}_0$ is the source current density vector, and ν and σ are the reluctivity and conductivity coefficients, respectively. Using the property of edge based finite element method [2], the following partial differential equation can be obtained

$$rot\,(\nu\, rot\mathbf{A}) + \sigma\,\frac{d\mathbf{A}}{dt} - \mathbf{J}_0 = 0\,. \qquad (3)$$

To solve the electromagnetic circuit (Fig. 1) driven by the supplied voltage, discretisation of both (3) as well as the following equation derived from Kirchoff's second law must be performed [3]

$$V_0 = \frac{d\Psi}{dt} + (R_0 + R_w)\,I_0 + L_0\frac{dI_0}{dt}\,, \qquad (4)$$

where Ψ is the interlinkage flux of the winding, V_0 is the supplied voltage from the network, I_0 is the current in the exciting winding, R_0 and L_0 neither of which are included in the finite element analysis region, are the resistance and the inductance of the lead wire and the load, respectively, while R_w is the DC resistance of the winding (Fig. 1). In (3), the current density vector $\mathbf{J}_0$ can be substituted by the current intensity value I_0 using the following equation

$$\mathbf{J}_0 = \frac{n_w}{S_w}\,I_0\,\mathbf{n}_0\,, \qquad (5)$$

where n_w and S_w are the number of turns and its cross sectional area, respectively, while $\mathbf{n}_0$ is the vector which represents flow direction of the current.

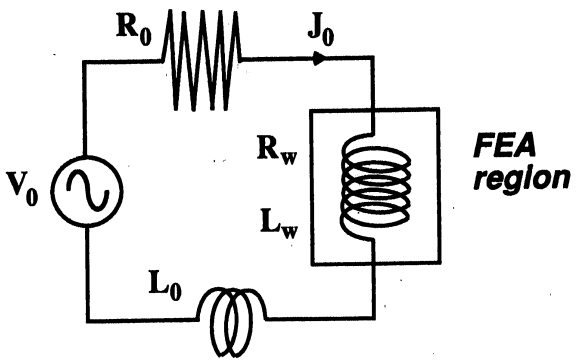

Fig. 1. Equivalent electromagnetic circuit

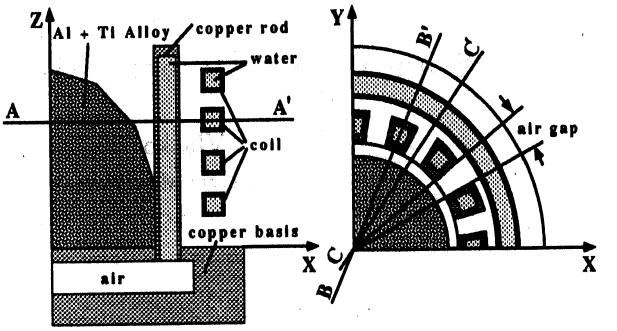

a) X-Z plane b) Cross section $A - A'$

Fig. 2. Analyzed model.

The interlinkage flux Ψ as a function of magnetic vector potential $\mathbf{A}$, can be obtained by the following equation

$$\Psi = \frac{n_w}{S_w} \int\int\int_v \mathbf{A} \cdot \mathbf{n}_0 \, dv \, . \tag{6}$$

Using a time-periodical voltage source expressed by the complex value V_0, we can substitute d/dt with $j\omega$ and obtain the following equation

$$V_0 = (R_0 + R_w + j\omega L_0) I_0 + j\omega \frac{n_w}{S_w} \int\int\int_v \mathbf{A} \cdot \mathbf{n}_0 \, dv \, . \tag{7}$$

Performed discretisation on both (3) and (7) leads to a set of linear algebraic equations with complex coefficients where magnetic vector potential $\mathbf{A}$ and source current I_0 are unknown values, while the supplied voltage source V_0 is a known variable

$$\begin{bmatrix} [\,S_{ij}\,] & [\,B_{ip}\,] \\ [\,B_{ip}\,]^T & [\,C_{pp}\,] \end{bmatrix} \begin{bmatrix} \{\,A_i\,\} \\ \{\,I_{0_p}\,\} \end{bmatrix} = \begin{bmatrix} \{\,0\,\} \\ \{\,V_{0p}\,\} \end{bmatrix} \tag{8}$$

$i, j = 1, \ldots, n$; $p = 1, \ldots, m$, where n is the number of edges, and m is the number of sources.

The above system of equation is generally asymmetrical but can be easily transformed into a symmetrical system by dividing the last p-rows with $j\omega$, which enables the use of the ICCG method for solving symmetrical matrices, thereby reducing computational time and memory requirements.

III. Analyzed Model and Obtained Results

A. Model

Fig. 2, shows the plane view and cross sections $A - A'$, $B - B'$ and $C - C'$ of one of the analyzed models. The shape of the aluminum and titanium alloy inside the furnace was predicted before performing the analyses using the experimental results. The purpose of the copper rods is to mechanically prevent molten alloy from leaking out of the furnace and to emphasize the value of magnetic flux density in the air gaps between rods. To avoid overheating, water is circulated inside the coils and the copper rods.

B. Eddy current losses

Eddy current losses in the conducting material having a conductivity σ can be computed using the following equation

$$P = \sum_{i=1}^{nel} \frac{1}{2} \left(\int\int\int_V \frac{1}{\sigma} \mathbf{J}_{ei} \, \mathbf{J}_{ei}^* \, dv \right) , \tag{9}$$

where nel is the total number of finite elements in the conductive material, $\mathbf{J}_{ei}$ and $\mathbf{J}_{ei}^*$ are the eddy current density vector and its conjugate value, respectively, while V is the volume of each finite element.

Because conductivity coefficients σ for copper and aluminum and titanium alloy differ to a great degree – copper's conductivity is about 40 times than that of the alloy – the amount of power consumed by each becomes important. Due to copper's high thermal and electric conductivities, the eddy current loss in copper rods is significant. The goal, therefore, in order to minimize the loss, is to optimize the number and position of the copper rods inside the furnace. We analyzed the power ratio between the copper rods and the alloy by varying the number of copper rods and therefore the size of the air gaps between them. We also analyzed the ratio between total input power into the system and the power consumed by the melting alloy alone. Fig. 3 shows the results. Figs. 4 and 5, show the magnetic flux density and eddy current distributions at cross section $A - A'$, for the furnace models with the smallest and the largest air gaps between rods, respectively. As the results indicate, the power ratio favors the molten alloy as the number of copper rods decreases and the air gap distance increases. An increase in the air gap between rods (Figs. 4 and 5) enables the magnetic flux to penetrate deeper into the furnace, increasing the power consumed by the alloy. Removing the copper rods altogether seems an ideal solution, but that would to abandon their main function.

C. Electromagnetic forces

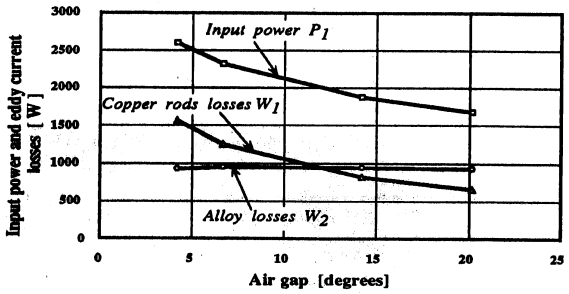

a) Input power and eddy current losses

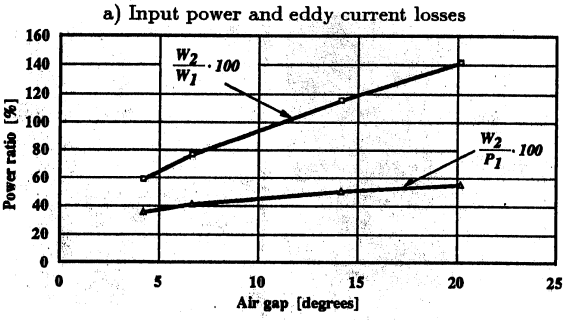

b) Power ratio

Fig. 3. Obtained results

In order to optimize the number and position of copper rods the analysis of electromagnetic force is also an important consideration. Using the *volume force density method*

$$\mathbf{F} = \int\int\int_v \mathbf{J}_e \times \mathbf{B}\, dv\,, \qquad (10)$$

the electromagnetic force vector $\mathbf{F}$ is computed. Figs. 6 and 7 express the distributions obtained for the largest and smallest air gaps. We considered three typical cross sections, $A - A'$, $B - B'$, $C - C'$ (see Fig. 2), where we displayed the electromagnetic force vector distribution:

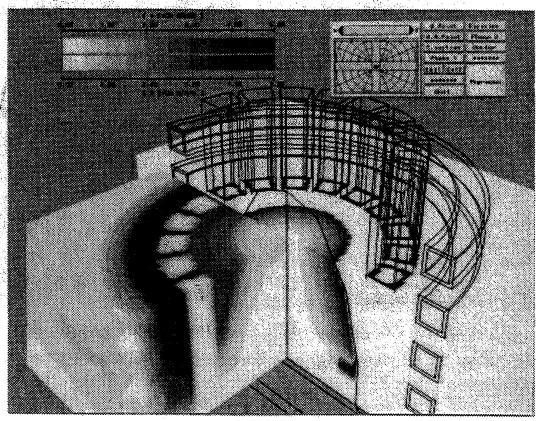

Fig. 4. Magnetic flux density and eddy current distributions for smallest air gap model

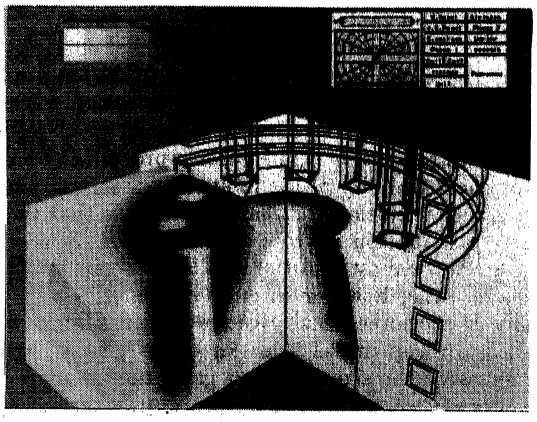

Fig. 5. Magnetic flux density and eddy current distributions for largest air gap model

1. Horizontal cross section $Z = const.$, $A - A'$,
2. Vertical cross section at mid-copper rod, $B - B'$,
3. Vertical cross section at mid-air gap, $C - C'$.

a) smallest air gap model

b) largest air gap model

Fig. 6. Electromagnetic force density distribution at cross section $A - A'$

It is clear from Figs. 6 and 7 that, the orientation of the electromagnetic forces inside the molten alloy is toward the furnace's central axis.

In addition, the intensity of the force density vectors $d\mathbf{f} = \mathbf{J}_e \times \mathbf{B}$ continually change, reaching their peak value in the air gap area (Fig. 6). It is possible to interpret, therefore, that the forces will keep the alloy inside of the

furnace even in the absence of the copper rods. This solution is best only when considering power efficiency but, due to the complexity of the system, the amount and shape of molten alloy are highly unpredictable function. Eliminating the copper rods would create problems in the control and regulation of the heating process, as well as in the physical stability of the molten alloy in the furnace.

Another conclusion that can be drawn is that the force density distribution in cross section $B - B'$ is nearly the same for the largest and the smallest air gap models. At the same time, however in cross section $C - C'$ the intensity of the force density vector is much larger for the smallest air gap model than for the largest. Therefore, by increasing the size of the air gaps, the intensity of the force density vector decreases, preventing the removal of all the copper rods. Instead, the number and position of the copper rods must be optimized, taking into account weight and amount of molten alloy in the furnace. This proposed method is highly applicable for designing the optimal shape of the analyzed furnace.

As reference, the ICCG "solver" was used to solve the algebraical system of equations. The computation was performed on a *Silicon Graphics IRIS Indigo 4000 (120 MIPS)* computer. All other relevant parameters are given in Table I.

TABLE I

Analysis data

air gap [degrees]	4.2	6.7	14.2	20.2
Number of nodes	6999	6252	4758	4011
Number of elements	39771	35352	26514	22095
Number of edges	47422	42241	31879	26698
Non-zero entries	699076	619120	458932	378958
CPU time [min]	19.85	18.36	11.12	7.52

Conclusion

In this paper, we analyzed the magnetic flux density, eddy current, and electromagnetic force distributions to produce a high-efficiency induction skull melting furnace. Using the edge-based finite element method and supplied voltage as a source, time-periodic finite element analyses were performed. The steady-state phenomena were obtained directly. The efficiency of the furnace depends to a great degree on the number and position of the copper rods and the size of the air gaps between them. It becomes possible, however, to optimize the number and the position of the copper rods by taking into consideration the electromagnetic forces, and the weight and amount of molten alloy.

Cross section $B - B'$

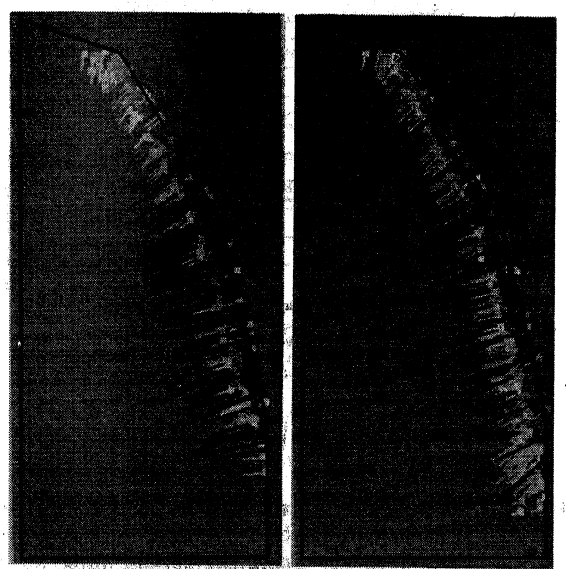

Cross section $C - C'$

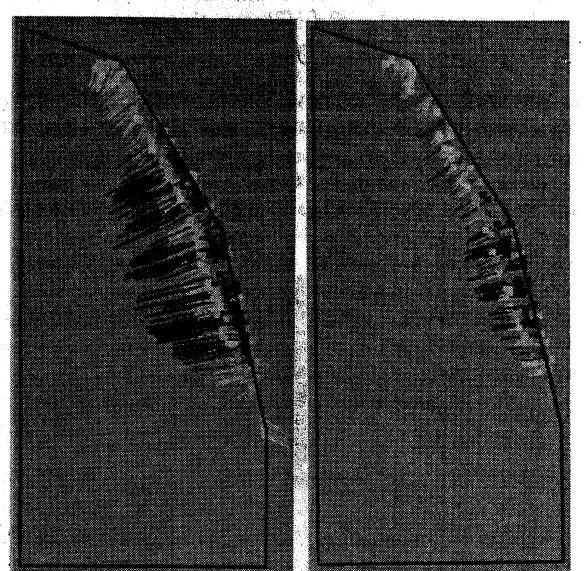

a) smallest air gap model b) largest air gap model

Fig. 7. Electromagnetic force density distribution

References

[1] J. D. Lavers, "Numerical solution methods for electroheat problems", *IEEE Trans. on Mag.* Vol. 19, No. 6, pp. 2566 - 2572, Nov. 1983.

[2] A. Kameari, "Three dimensional eddy current calculation using edge elements for magnetic vector potential", *Proceedings of the First International Symposium in Applied Electromagnetics in Materials, Tokyo*, 3-5 October 1988.

[3] T. Nakata, N. Takahashi, K. Fujiwara and A. Ahagon, "3-D finite element method for analyzing magnetic fields in electrical machines excited from voltage sources", *IEEE Trans. on Mag.* Vol. 24, No. 6, pp. 2582 - 2584 Nov. 1988.